Theoretical Study of OH−O 2 −Isoprene Peroxy Radicals

ARTICLE *in* THE JOURNAL OF PHYSICAL CHEMISTRY A · JANUARY 2001

Impact Factor: 2.69 · DOI: 10.1021/jp0027039

Theoretical Study of OH−O_2−Isoprene Peroxy Radicals

Wenfang Lei and Renyi Zhang*

Department of Atmospheric Sciences, Texas A&M University, College Station, Texas 77843

W. Sean McGivern, Agnes Derecskei-Kovacs, and Simon W. North*

Department of Chemistry, Texas A&M University, College Station, Texas 77843

Received: July 27, 2000; In Final Form: October 31, 2000

Ab initio molecular orbital calculations have been performed to investigate the structures and energetics of the peroxy radicals arising from the OH-initiated oxidation of isoprene. Geometry optimizations of the OH−O_2−isoprene peroxy radicals were performed using density functional theory at the B3LYP/6-31G** level, and individual energies were computed using second-order Møller−Plesset perturbation theory (MP2) and coupled-cluster theory with single and double excitations including perturbative corrections for the triple excitations (CCSD(T)). At the CCSD(T)/6-31G* level of theory the zero-point-corrected OH−O_2−isoprene adduct radical energies are 47−53 kcal mol^{-1} more stable than the separated OH, O_2, and isoprene reactants. In addition, we find no evidence for an energetic barrier to O_2 addition and have calculated rate constants for the O_2 addition step using canonical variational transition state theory (CVTST) based on Morse potentials to describe the reaction coordinate. These results provide the isomeric branching between the six isoprene−OH−O_2 adduct radicals.

I. Introduction

Hydrocarbons play an important role in atmospheric chemistry.[1,2] Photochemical oxidation of hydrocarbons results in a number of compounds that have major implications for local and regional air quality, acid deposition, and the greenhouse effect including ozone (O_3), acid, and carbon dioxide (CO_2) production.[3] Isoprene (2-methyl-1,3-butadiene, $CH_2{=}C(CH_3)$-$CH{=}CH_2$) is one of the most abundant hydrocarbons emitted by the terrestrial biosphere with a global average production rate of ∼450 Tg yr^{-1} and is sufficiently reactive to influence oxidation levels over large portions of the continental troposphere.[4,5] Many deciduous trees emit ∼1% of the CO_2 fixed during photosynthesis as isoprene. Biogenic isoprene comprises a hydrocarbon source that exceeds the emission of the nonmethane hydrocarbons of anthropogenic origin,[6] and an accurate and complete knowledge of the atmospheric chemistry of isoprene is critical to the elucidation of chemical mechanisms in urban and regional environments.

Atmospheric oxidation reactions of isoprene are initiated by an attack from the hydroxyl radical, OH, ozone, O_3, or the nitrate radical, NO_3. Since isoprene is emitted from vegetation only during daylight hours, the reaction with OH is expected to be the dominant tropospheric removal pathway for isoprene. The reaction between isoprene and OH occurs almost entirely by OH addition to the >C=C< bonds, yielding four possible hydroxyalkyl radicals. Under atmospheric conditions, the hydroxyalkyl radical reacts primarily with oxygen molecules to form hydroxyalkyl peroxy radicals. In the presence of nitric oxide NO, the subsequent reaction of the hydroxyalkyl peroxy radicals leads to the formation of hydroxyalkoxy radicals. The dominant tropospheric reaction of hydroxyalkoxy radicals is believed to be decomposition, leading to the formation of various oxygenated and nitrated organic compounds. Figure 1 shows a mechanistic diagram for the formation of the four OH−isoprene adducts and the six corresponding peroxy radicals.

The oxidation reactions of isoprene initiated by OH have been the subject of numerous studies.[1,7] Several laboratory experiments have reported rate constants of isoprene with OH[8−17] and have identified several major reaction products, including α,β-unsaturated carbonyls (methyl vinyl ketone and methacrolein), formaldehyde, and organic nitrates.[18−27] Recently, two theoretical studies have investigated the equilibrium structures and energetics of the OH−isoprene adduct radicals.[28,29] At present, however, direct experimental data concerning the intermediate steps in the oxidation mechanism are still sparse. Both the isomeric branching in the addition of OH to isoprene and subsequent O_2 addition rates determine the final branching ratios for the peroxy radicals. Two recent models for the atmospheric degradation of isoprene employ significantly different peroxy radical branching ratios.[27,30] The model of Jenkin and Hayman[30] predicts a strong propensity for only a few isomers in contrast to the model of Paulson and Seinfeld[27] which predicts that all six peroxy isomers are formed in comparable yields. The resolution of this discrepancy is central to the present study.

In this work, we report ab initio calculations on the peroxy radicals arising from the OH-initiated oxidation reaction of isoprene. The equilibrium structures of the OH−O_2−isoprene peroxy radicals have been calculated using density functional theory, and the energetics were calculated for each stationary point using MP2 and CCSD(T) theories with different basis sets. We have also performed calculations using the canonical variational transition state theory to determine the rate constants associated with O_2 addition to the OH−isoprene peroxy radicals based on the ab initio binding energies. The calculated rate constants provide the relative isomeric branching between the six peroxy radicals and, when combined with our previous

* Corresponding authors.

10.1021/jp0027039 CCC: $20.00
Published on Web 12/15/2000

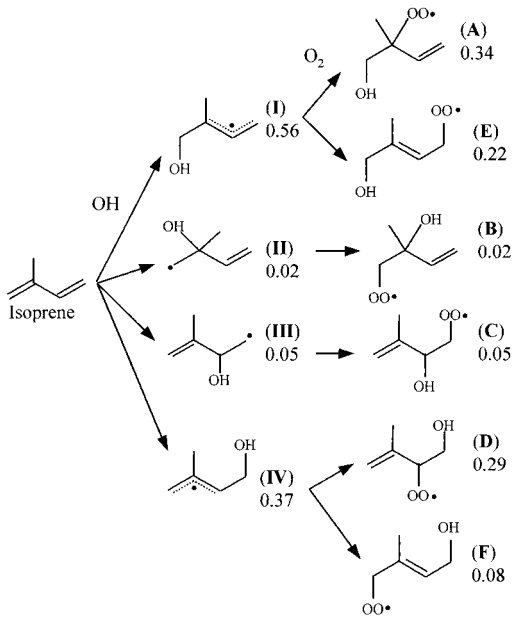

Figure 1. Mechanistic diagram for the reactions of isoprene in the presence of OH and O_2. The numbers label the branching ratios for each reaction pathway.

results for the formation of the isoprene−OH adduct, the overall branching.

II. Theoretical Approach

Ab initio molecular orbital calculations were performed on an SGI Origin 2000 supercomputer using the Gaussian 98 software package.[31] Previous benchmarking calculations on the isoprene−OH adducts have identified a level of ab initio theory suitable for calculations on these systems on the basis of efficiency and accuracy for complex organic radicals, and these results have been extended to the present calculations on the isoprene−OH−O_2 adducts.[29] The results indicated that density functional and MP2 methods yielded very similar geometries but considerably higher computational efficiency and faster convergence were achieved using the gradient-corrected density functional theory in geometry optimizations and frequency calculations. Little improvement in the molecular geometry was observed when the size of the basis set was increased above the polarized double-zeta level. As a result, we have adopted the following methods in the present calculations. Geometry optimizations were performed using Becke's three-parameter hybrid method employing the LYP correction function (B3LYP) in conjunction with a split-valence polarized basis set, 6-31G**. Vibrational frequency calculations were also performed at the same level in order to obtain zero point correction energies. Single-point energy calculations were then carried out using second-order Møller−Plesset perturbation theory (MP2) and coupled-cluster theory with single and double excitations including perturbative corrections for the triple excitations (CCSD(T)) using different basis set sizes.

III. Results and Discussion

Geometries of OH−O_2−Isoprene Peroxy Radicals. For the OH−isoprene adduct, the addition of O_2 occurs only at the carbons β to the OH position for radicals **II** and **III**, but takes places at two centers (β or δ to the OH position) for radicals **I** and **IV**. Hence O_2 addition to the OH−isoprene adduct results in the formation of six peroxy radical isomers (Figure 1). For each structural isomer, we have performed calculations to explore possible (typically five to six) rotational conformers. A total of about 30 rotational conformations were considered, and we report the lowest rotational conformer found for each structural isomer. The lowest-energy conformers of the six peroxy radicals are shown in Figure 2. The evaluation of the vibrational frequencies[32] confirmed that all geometries reported here represent minima on the potential energy surfaces.

TABLE 1: Calculated Total Energy (in hartrees) at the B3LYP/6-31G Optimal Geometries (see Figure 2) for the OH−O_2−Isoprene Peroxy Radicals at Different Levels of Theory**

isomer	MP2/6-31G*	MP2/6-311++G**	CCSD(T)/6-31G*
A	420.159 202	420.430 181	420.270 046
B	420.159 024	420.430 047	420.270 380
C	420.156 112	420.427 718	420.267 405
D	420.154 542	420.427 957	420.267 032
E	420.151 372	420.424 087	420.261 874
F	420.149 728	420.423 057	420.260 288

The geometries shown in Figure 2 can be compared to the isoprene−OH adduct geometries calculated previously.[29] For peroxy radicals **A** and **D**, addition of O_2 to the OH-isoprene adduct results in a shortening of the C−O(H) bond, whereas this C−O(H) bond length is nearly unchanged in radicals **E** and **F**. The C−C bond lengths adjacent to the site of O_2 addition are increased, as electron density in the π bond is transferred to the newly formed C−O bond. For example, addition of O_2 to carbon 2 for the OH−isoprene adduct **I** increases the C−C carbon bond lengths by 0.04 and 0.11 Å for C1−C2 and C3−C4 bonds, respectively. The C−C carbon length associated with the methyl substituent is also increased by about 0.03 Å. On the other hand, the C3−C4 bond length between carbons 3 and 4 is reduced by about 0.05 Å. Similar changes in the C−C bond characteristics occur for all radicals upon O_2 addition.

Energetics of OH−O_2−Isoprene Peroxy Radicals. The total energies of the OH−O_2−isoprene adduct isomers were determined using the B3LYP/6-31G** optimized geometries at the MP2 and CCSD(T) levels with different basis sets and the results are shown in Table 1. The zero-point-corrected energies relative to the separated O_2, OH, and isoprene reactants reveal that both the level of electron correlation and the size of the basis set have a significant impact on the energetics. For the six isomers of the OH−O_2−isoprene adduct, the relative energies computed at the MP2 level of theory are systematically higher using a larger basis set size (i.e., 6-311++G**). For isomers **D**, **E,** and **F** the relative energies obtained using the basis sets of 6-31G* and 6-311++G** differ by 0.6, 1.0, and 0.6 kcal mol^{-1}, respectively, while for isomers **A, B,** and **C** the relative energies calculated using the two basis sets differ by 1.7, 2.1, and 2.1 kcal mol^{-1}, respectively. Also, using the basis set of 6-31G*, the highly correlated method (i.e., CCSD(T)) produces consistently lower relative energies compared to the MP2 method, with the largest relative energy difference of about 2.5 kcal mol^{-1}. Table 2 reveals that the most energetically favorable peroxy radicals with respect to separated products are those with OH addition to C1 and C2 positions and subsequent O_2 addition to C2 and C1 positions. The relative stability of the peroxy radicals is almost independent of basis set and electron correlation effects: isomers **A** and **B** have the lowest energies and isomers **E** and **F** have the highest energies (by about 5−6 kcal mol^{-1} higher than radicals **A** and **B**). Note that the relative stability of the OH−O_2−isoprene peroxy radicals (i.e., with respect to the separate OH, O_2, and isoprene reactants) should be distinguished from their binding energies relative to the OH−isoprene adduct precursors. It is the bending energies that ultimately influence the O_2 addition rates.

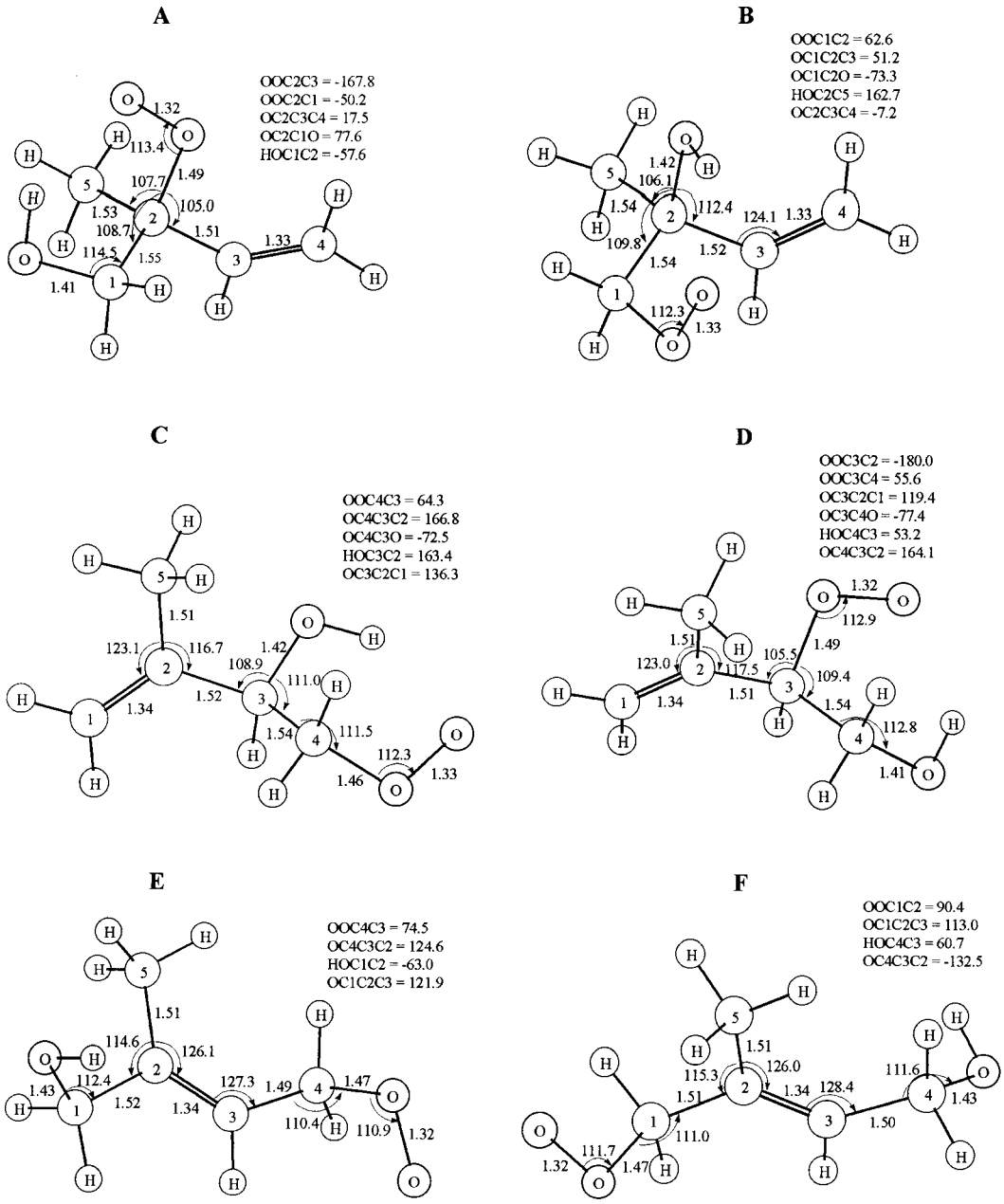

Figure 2. Optimized geometries of the six isomers of the isoprene−OH−O_2 adduct calculated at the B3LYP/6-31G** level of theory (bond lengths in angstroms and angles in degrees).

TABLE 2: Zero-Point-Corrected Relative Energies[a] (kcal mol^{-1}) for the OH−O_2−Isoprene Peroxy Radicals

	MP2		CCSD(T)	
isomer	6-31G*	6-311++G**	6-31G*	6-31G*+CF[b]
A	52.8	50.7	54.3	52.2
B	52.7	50.6	54.4	52.4
C	50.7	49.0	52.4	50.7
D	49.7	49.1	52.2	51.6
E	47.6	46.6	48.8	47.8
F	46.6	46.0	47.9	47.3

[a] Energy difference between the peroxy radicals and the reactants (i.e., OH + O_2 + isoprene). Zero point energy (ZPE) corrections calculated at the B3LYP/6-31G** level; all geometries calculated at the B3LYP/6-31G** level of theory. [b] Correction factor (see text for details).

The results from Table 2 suggest that highly correlated methods, along with large basis sets, are necessary for accurate energy calculations of the peroxy radicals of the OH−isoprene reaction system. For the OH−O_2−isoprene peroxy radicals, single-energy calculations at the CCSD(T) level of theory using a larger basis set (e.g., 6-311++G**) are computationally prohibitive. Therefore, we have attempted to correct for basis set effects for the isomers of the OH−O_2−isoprene peroxy radicals based on an approach that has been recently developed and employed to investigate the bond dissociation energies of haloalkanes using correlation consistent basis sets.[33] A similar correction has been applied to a determination of the energetics for the OH−isoprene adduct isomers.[29] The procedure involved determination of a correction factor associated with basis set effects at the MP2 level and subsequent correction to the energy calculated at a higher level of electron correlation with a moderate size basis set. For the isomers of the OH−O_2−isoprene adduct, basis set effects on the relative energies were evaluated at the MP2 level. A correction factor, CF, was determined from the calculated relative energy difference between the MP2/6-31G* and MP2/6-311++G** levels. The values of calculated

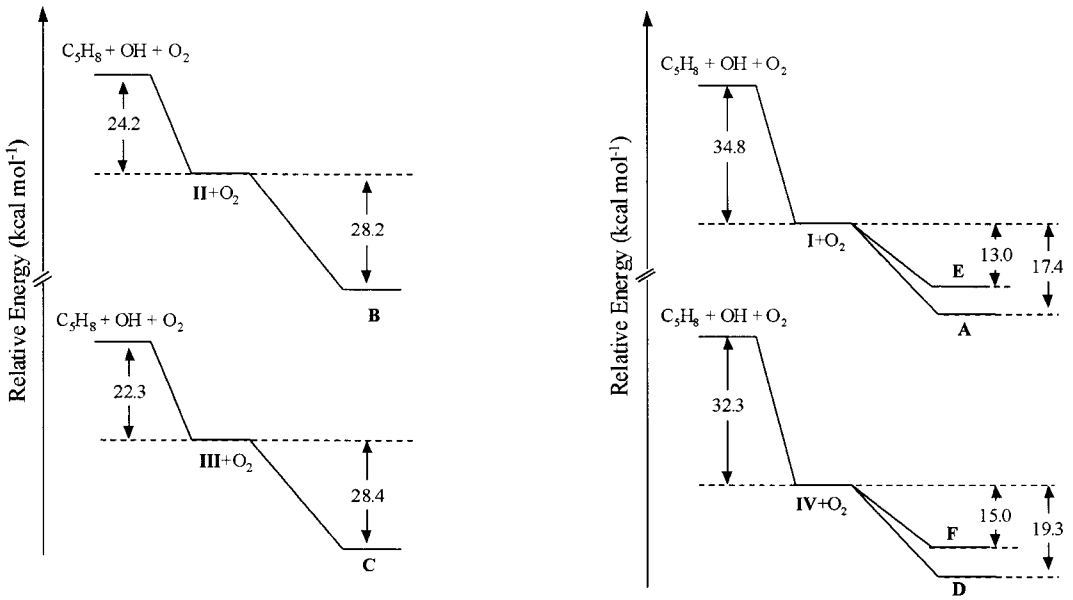

Figure 3. Schematic energy diagram for the OH−O_2-isoprene reaction system for OH−isoprene adducts **I** to **IV** resulting in peroxy radicals **A** to **F**. The energies for the OH−isoprene adduct and OH−O_2−isoprene adduct were obtained at the CCSD(T)/6-311G** and CCSD(T)/6-31G* + CF levels of theory, respectively.

energies at the CCSD(T)/6-31G* level were then corrected by the MP2 level correction factor. The correction factors are in the range of 0.6−2.1 kcal mol^{-1} for the isomers of the OH−O_2−isoprene peroxy radicals. Table 2 summarizes zero-point-corrected relative energies of the OH−O_2−isoprene peroxy radicals obtained using the various methods. At the CCSD(T)/6-31G* + CF level of theory, the peroxy radicals are 47.3−52.4 kcal mol^{-1} more stable than the separated reactants (i.e., OH + O_2 + isoprene). A schematic energy diagram involving the six peroxy isomers **A** to **F** of the OH−O_2−isoprene reaction system is shown in Figure 3. The values for the energies of the OH−isoprene adduct isomers are taken from ref 29. We estimated an uncertainty of ±1 kcal mol^{-1} associated with the energetics of the OH−O_2−isoprene peroxy radicals, based on a validation study for similar radical species.[29]

We have also calculated the standard heats of formation for the lowest energy isomers, estimated from the calculated total energies (E), the experimentally known heats of formation for the reactants, and thermal energy correction (TC). The enthalpy of reaction (ΔH_{rxn}) for the addition of OH and O_2 to isoprene at 298 K to form the peroxy radical isomers is expressed by

$$\Delta H_{rxn} = [E(C_5H_8OH(O_2)) - E(C_5H_8) - E(O_2) - E(OH)] + [TC(C_5H_8OH(O_2)) - TC(C_5H_8) - TC(O_2) - TC(OH)] \quad (1)$$

where the thermal energy corrections were made using frequencies calculated at the B3LYP/6-31G**level. The heat of formation for each peroxy radical can be obtained directly from the corresponding enthalpy of reaction

$$\Delta H_{rxn} = \Delta H_f^0(C_5H_8OH(O_2)) - \Delta H_f^0(C_5H_8) - \Delta H_f^0(O_2) - \Delta H_f^0(OH) \quad (2)$$

using experimentally determined heats of formation for the isoprene, OH and O_2.[34] The values of the calculated heats of formation of the OH−O_2−isoprene peroxy radicals are also listed in Table 3 using relative energies evaluated at two different levels of theory. The uncertainty in our calculated heats of formation is approximately ±1 kcal mol^{-1}, similar to the uncertainty associated with the energetics of the peroxy radicals, since the uncertainty of the experimental heats of formation for O_2, isoprene and OH are minor.

TABLE 3: Calculated Standard Heats of Formation (kcal mol^{-1}) for the OH−O_2−Isoprene Peroxy Radicals

isomer	$\Delta H_f^{0\,a}$	$\Delta H_f^{0\,b}$
A	24.2	26.9
B	24.2	27.2
C	22.5	24.6
D	22.6	26.1
E	19.8	22.4
F	19.2	21.5

[a] Based on zero-point-corrected energies calculated at the MP2/6-311++G**//B3LYP/6-31G** level of theory. [b] Based on zero-point-corrected energies calculated at the CCSD(T)/6-31G+CF*//B3LYP/6-31G** level of theory.

Rate Constant Calculations. The high-pressure rate constants for the dissociation of the $C_5H_8OH(O_2)$ adducts were evaluated using canonical variational transition state theory (CVTST). The dissociation rates were converted to the association rates via the equilibrium constant:

$$\frac{k_{rec}}{k_{uni}} = K_{eq} = \frac{Q_{AB}}{Q_A Q_B} \exp\left(\frac{\Delta E}{kT}\right) \quad (3)$$

where Q_{AB} is the partition function of the adduct, Q_A and Q_B are the partition functions of the individual products, and ΔE is zero-point corrected reaction energy. The bimolecular rate is given by

$$k_{uni} = \frac{kT}{h} \frac{Q^{\ddagger}_{AB}}{Q_{AB}} \exp\left(-\frac{\Delta E}{kT}\right) \quad (4)$$

where $Q^{\ddagger}_{AB}$ is the partition function of the transition state with the vibrational frequency corresponding to the reaction coordinate removed, Q_{AB} is the partition function of the adduct, and ΔE is the zero-point-corrected transition state energy relative to the separated reactants.

The partition functions required for eqs 3 and 4 were calculated by treating the rotational and translational motion

TABLE 4: CVTST Calculated High-Pressure Formation Rate Constants for the OH−O_2−Isoprene Peroxy Radicals

isomer	rate of formation (cm^{-3} $molecule^{-1}$ s^{-1})
A	1.58×10^{-12}
B	1.53×10^{-12}
C	1.42×10^{-12}
D	4.61×10^{-13}
E	1.07×10^{-12}
F	1.29×10^{-13}

classically and treating vibrational modes quantum mechanically. Unscaled vibrational frequencies and moments of inertia for the isoprene−OH adducts were taken from recent ab initio calculations at the B3LYP/6-31G** level.[29] Frequencies and moments of inertia for the peroxy radicals were obtained at the B3LYP/6-31G** level as discussed previously. The reaction energies were taken to be zero-point-corrected energies calculated at the CCSD(T)/6-311G**// B3LYP/6-31G** level. The conserved modes of the transition state were assumed to resemble the product modes.[35] The dependence of the transitional mode frequencies with C−O(O) distance were modeled using[36]

$$\nu(r) = \nu_0 \exp[-a(r - r_e)] + B \qquad (5)$$

where ν_0 is the vibrational frequency in the reactant molecule, r_e is the equilibrium bond distance, B is the sum of the rotational constants of the individual isoprene−OH adduct and O_2 molecules, and a is a constant. Moments of inertia at fixed geometries were calculated by changing only the C−O(O) distance. The potential energy surface along the reaction coordinate was modeled by a Morse function including the centrifugal barrier

$$V(r) = D_e[1 - \exp(-\beta r)]^2 + B_{ext}(r)J(J+1) \qquad (6)$$

where D_e is the bond dissociation energy, $B_{ext}(r)$ is the external rotational constant determined by assuming that the molecular was a symmetric top, and J was assumed to be the average rotational quantum number of a Boltzmann distribution calculated using the external rotational constant of the molecule at the equilibrium configuration.

The individual rates of formation of each isomer were obtained using eqs 4 and 6, variationally minimizing the rate as function of the C−O(O) bond distance. The value of a was determined to be 1.15 $Å^{-1}$ based on a functional fit to the r dependence of the transitional frequencies evaluated at the B3LYP/3-21G* level of theory. This assumes that the largest change in ZPE is due to the decrease in transitional mode frequencies and, therefore, provides an effective dependence of these modes on bond length. The results of the CVTST calculations are shown in Table 4 for each peroxy isomer. The values of the high-pressure rate constants fall in the range of 1×10^{-12} to 1×10^{-13} cm^3 $molecule^{-1}$ s^{-1}, significantly faster than the corresponding rates associated with O_2 addition to aromatic−OH adducts but slower than the reaction of O_2 with alkyl and hydroxyalkyl radicals. The addition rates to form isomers **A**, **B**, **C**, and **E** are comparable while the addition rates to form isomers **D** and **F** are much slower. Although all isoprene−OH adduct isomers will react rapidly with O_2 under ambient conditions, the relative rates between the formation of isomers **A** and **E** and between **D** and **F** will influence final product branching ratios in the oxidation of isoprene. We find that the **A**:**E** and **D**:**F** relative branching ratios are 0.60:0.40 and 0.78:0.22, respectively. Table 5 shows the peroxy radical branching ratios based on the present calculations and the results from refs 27 and 30. A strong preference for isomers A, E, and D is predicted in good agreement with the model of Jenkin and Hayman[30] but qualitatively different from the model of Paulson and Seinfeld.[27] Jenkin and Hayman suggested the branching ratios based on the assumption that the peroxy radical center would form at the more substituted site.[30] Hence our CVTST calculations indicate that the calculated branching ratios and rate constants of the peroxy radicals are mostly dependent on their binding energies and the nature of the transition states, but not on their relative stability. For the peroxy radicals the relative stability is very different from the binding energy, because of the different binding energies for the four OH−isoprene adduct isomers.

TABLE 5: CVTST Calculated Branching Ratios for the Reaction of OH−Isoprene Adduct Radical with O_2 and Comparison with Previously Suggested Values

peroxy radical	calcd branching ratio	Jenkin and Hayman[a]	Paulson and Seinfeld[b]
A	0.34	0.45	0.212
E	0.22	0.15	0.141
B	0.02	0.05	0.236
C	0.05	0.05	0.164
D	0.29	0.23	0.123
F	0.08	0.08	0.123

[a] Reference 30. [b] Reference 27.

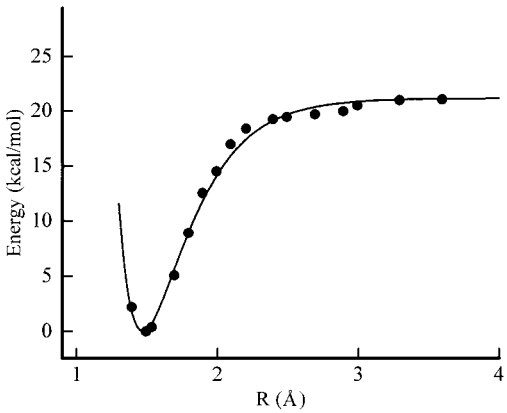

Figure 4. Potential energy as a function of C−O(O) distance for isomer **A** of the OH−O_2−isoprene radical. The symbols are obtained from the single energy calculations using B3LYP/6-31G**//B3LYP/3-21G* for fixed C−O(O) bond lengths. The solid curve is the calculated Morse potential from the binding energy and equilibrium C−O(O) stretching vibrational frequency.

In order to evaluate the absolute and relative rates of O_2 addition to the isoprene−OH adduct we must characterize the form of the potential along the reaction coordinate, specifically, whether there is a well-defined transition state or the addition proceeds without a barrier via a loose transition state. A characterization of the transition states associated with O_2 addition to aromatic−OH adducts has been recently performed by Andino et al.[37] The authors employed a constrained optimization procedure, using geometry optimizations at fixed C−O(O) bond lengths using the UHF/PM3 level; once the energy maximum along this coordinate was located, single-point calculations were performed at the B3LYP/6-31G** level of theory to obtain a better estimate of the barrier height. We have chosen to follow a similar procedure, but performing geometry optimizations at the B3LYP/3-21G* level of theory for fixed C−O(O) bond lengths. The results of calculations for the addition of O_2 to isoprene−OH adduct **I** to give peroxy isomer **A** are illustrated in Figure 4. We find no energy that exceeds the bond dissociation energy along the reaction coordinate in

contrast to the results of the addition of O_2 to aromatic−OH adducts.[37] The β parameter for the Morse potential in eq 6 is given by $\beta = (2\pi^2\mu/D_e)^{1/2}\nu$, where μ is the reduced mass of the bonded atoms, D_e is the bond dissociation energy, and ν is the vibrational frequency of the reaction coordinate in the parent molecule.[38] In order to test the applicability of this functional form to the present system, we have calculated the β parameter for isomer **A** using the binding energy and C−O(O) stretching frequency calculated at the B3LYP/3-21G* level. The Morse potential derived from this parameter is shown as the solid line in Figure 4 and is in good agreement with the B3LYP calculations. Although the B3LYP/3-21G* calculations do not reproduce the high-level ab initio binding energies, we believe they correctly describe the qualitative features of the potential. The good agreement between the calculated B3LYP/3-21G* reaction coordinate and the Morse potential derived from eq 6 provides strong evidence that the functional form used to model the reaction coordinate is reasonable. The individual β parameters used in the CVTST calculations for the six isomers were derived using the high-level ab initio binding energies and vibrational frequencies for each species.

Recently, two theoretical studies have investigated the energetics and isomeric branching for the initial addition of OH to isoprene.[28,39] Although the energetics calculated by Stevens et al. (ref 28) and Lei et al. (ref 39) are similar, the conclusions of each study differ significantly. Stevens et al. report that, despite the large differences in binding energies, there should be an approximately equal distribution of all four adducts based on mass spectroscopic data for the fragmentation products of the OH−isoprene adduct isomers. This conclusion is inconsistent with the majority of previous studies on OH reactions with olefins,[11,40] mechanistic models for isoprene oxidation,[30] and the predictions of canonical variational transition state theory. In contrast, Lei et al. (ref 39) have reported that the formation rates for the four isomers are very different with OH addition to the two outer carbon positions dominating addition to the inner positions in agreement with previous estimates.

The sensitivity of the rate constants shown in Table 4 to the binding energies was examined by recalculating the rate constants for the six peroxy isomers using well depths which differed by ±3 kcal mol^{-1} from the present ab initio energies. In both cases, the individual rates changed by less than a factor of 2.5. In addition, the relative branching between isomers **A** and **E** differed by less than ±7% with a ±3 kcal mol^{-1} change in binding energy, though the branching between isomers **D** and **F** showed a slightly larger change (0.77 ± 0.05:0.24 ± 0.05). The relatively small sensitivity of the rate constants to large changes in the binding energies provides evidence that the reaction coordinate can be adequately described by a Morse potential.

We now briefly address the choice of a Morse function to model reaction coordinate. Bayes and co-workers have found that the rates predicted using the adiabatic channel model with a Morse potential were good to within an order of magnitude of experimental results.[41,42] The results were much better than using a long-range C_6 term but neither could reproduce the strong correlation of the rate constant with radical ionization potential.[41,42] The authors assumed a barrierless potential function developed to mimic the observed experimental trend. The functional form described a perturbation at long range due to an interaction with the charged state, $R^+ + O_2^-$:

$$V(r) = -\frac{H^2}{(\mathrm{IP} - \mathrm{EA}) - e^2/r} + \frac{H^2}{(\mathrm{IP} - \mathrm{EA})} \qquad (7)$$

where IP − EA is the difference between the ionization potential of the radical and the electron affinity of the O_2. The interaction matrix element, H, was varied to give good agreement with experiment. There was limited thermodynamic information available regarding the RO_2 adduct but it is unlikely that refined values would alter the final Morse results significantly. The authors and others,[43] however, note that the correlation does not apply to nonalkyl radicals like benzyl and allyl (C_3H_5).

Our calculated O_2 addition rates to the isoprene−OH adduct isomers are much closer in magnitude to the O_2 addition to alkyl radicals than to aromatic−OH adducts.[44] The high-pressure rates for addition of O_2 to alkyl radicals are fast, ranging from 2.2×10^{-12} cm^3 molecule^{-1} s^{-1} for CH_3 (refs 41 and 45) to 2.5×10^{-11} cm^3 molecule^{-1} s^{-1} for t-C_4H_9 (ref 41). The binding energies associated with O_2 addition to alkyl radicals are all approximately 30 kcal mol^{-1}.[46] The O_2 addition rates for hydroxyalkyl radicals are similar, ranging from 3.7×10^{-11} cm^3 molecule^{-1} s^{-1} for $CH_3C(OH)CH_3$ to 3.8×10^{-12} cm^3 molecule^{-1} s^{-1} for $CH_3CH(OH)CH_2$.[47] The rates for the β-hydoxyalkyl radicals are similar to the corresponding alkyls radicals while O_2 addition to the α-hydroxyalkyl radicals are faster. In contrast, the addition reactions involving aromatic−OH adducts are significantly slower. Estimates of $(2.1 \pm 0.2) \times 10^{-15}$ cm^3 molecule^{-1} s^{-1} by Bohn and Zetzsch[48] for the reaction of the benzene−OH adduct with O_2 and $<1 \times 10^{-15}$ cm^3 molecule^{-1} s^{-1} for the reaction of the toluene−OH adduct with O_2 have been reported.[49] The slower reaction rates of the aromatic−OH adducts are consistent with the lower binding energy associated with O_2 addition. This is not surprising considering the relative binding energies associated with the two classes of reactions. For the alkyl cases the binding energies are −32.7 kcal mol^{-1} for CH_3 and −35.5 kcal mol^{-1} for $C_2H_5O_2$.[46,50] The O_2 binding energies with hydroxyl radicals are slightly lower; for example, binding energies for $CH_3CH(OH)CH_2O_2$ and $CH_3CH(O_2)CH_2OH$ of −26.4 and −28.6 kcal mol^{-1}, respectively, have been recently calculated.[51] Binding energies for the aromatics−OH adducts with O_2, however, are much smaller. Garcia-Cruz et al. have recently obtained a value of 1 kcal mol^{-1} for the stability of the toluene−OH−O_2 adduct[52] and Andino et al. have reported ∼3 kcal mol^{-1} for the stability of the toluene−OH−O_2 adduct using density function theory.[37] These results are in agreement with other DFT calculations which estimate a 1.1 kcal mol^{-1} binding energy.[53] Temperature-dependent measurements indicate the presence of a small barrier, $E_a = 2$ kcal mol^{-1}, to O_2 addition, consistent with theoretical calculations albeit much lower.

Based on our calculated binding energies of O_2 with the four isoprene−OH adducts, it is likely that the addition rates are intermediate between the alkyl and aromatic analogues, as predicted by the CVTST calculations. A rate constant of $(6 \pm 2) \times 10^{-13}$ cm^3 molecule^{-1} s^{-1} at 296 ± 2 K has been measured for the reaction of the analogous allyl radical with O_2, close to our calculated result.[54] There are only two previously reported rate constants for O_2 addition to the isoprene−OH adduct. Zetzsch and co-workers have reported a value of 2.0×10^{-12} cm^3 molecule^{-1} s^{-1} at 300 K based on OH cycling experiments.[55] The result, although obtained indirectly, is in agreement with the present calculations. A more recent measurement of the rate constant of the isoprene−OH adduct with O_2, obtained by directly observing and monitoring the formation of the isoprene−OH adduct radical using the chemical ionization mass spectrometry (CIMS) approach, has determined a rate constant of about $(2.8 \pm 0.7) \times 10^{-15}$ cm^3 molecule^{-1} s^{-1}.[17] This rate constant is significantly smaller than those predicted by our

CVTST calculations, although are slightly higher than those of O_2 addition to OH−aromatic adducts. The origin of this discrepancy is unclear and we are currently performing additional experimental and theoretical studies to better define the addition reaction of O_2 to the isoprene−OH adduct. In particular, we are currently developing detection schemes for the peroxy radicals, which should provide valuable additional information to this system.

IV. Conclusions

In this paper we have presented ab initio molecular orbital calculations to investigate the structures and energetics of the peroxy radicals arising from the OH-initiated oxidation of isoprene. Equilibrium structures and energetics of the OH−O_2−isoprene peroxy radicals were investigated. At the CCSD(T)/6-31G* level of theory corrected for zero-point energy (ZPE), the OH−O_2−isoprene adduct radicals are about 47−53 kcal mol^{-1} more stable than the reactants. The energy barriers associated with O_2 addition to the OH−isoprene adduct radicals were found to be negligible, and the corresponding rate constants were calculated using canonical variational transition state theory (CVTST), with values in the range of 1×10^{-13} to 2×10^{-12} cm^3 $molecule^{-1}$ s^{-1}.

Acknowledgment. Financial support for this work was provided by the Texas Advanced Research Program (ARP) and The Texas A&M University Supercomputing Facilities. W.L. was supported by a graduate fellowship provided by a Grant from the Robert A. Welch Foundation (A-1417). The authors are grateful to Dr. Joe Francisco of Purdue University for helpful discussions and wish to acknowledge M. Clark Church for assistance in kinetic modeling. The authors also acknowledge the use of Laboratory for Molecular Simulations at Texas A&M.

References and Notes

(1) Atkinson, R. *J. Phys. Chem. Ref. Data Monogr*. **1994**, *2*, 1.
(2) Seinfeld, J. H.; Pandis, S. N. *Atmospheric Chemistry and Physics: From Air Pollution to Climate Change*; John Wiley & Sons: New York, 1997.
(3) IPCC Scientific Assessment, Climate Change; Cambridge University Press: 1992.
(4) Rasmussen, R. A.; Khalil, M. A. *J. Geophys. Res*. **1988**, *93*, 1417.
(5) Trainer, M., et al. *Nature* **1987**, *329*, 705.
(6) Placet, M.; Battye, R. E.; Fehsenfeld, F. C.; Bassett, G. W. In "NAPAP SOST Report 1"; National Acid Precipitation Assessment Program, Washington DC, 1990.
(7) Atkinson, R. *J. Phys. Chem. Ref. Data* **1997**, *26*, 251.
(8) Cox, R. A.; Derwent, R. G.; Williams, M. R. *Environ. Sci. Technol*. **1980**, *14*, 57.
(9) Kleindienst, T. E.; Harris, G. W.; Pitts, Jr., J. N. *Environ. Sci. Technol*. **1982**, *16*, 844.
(10) Atkinson, R.; Aschmann, S. M.; Winer, A. M.; Pitts, J. N., Jr. *Int. J. Chem. Kinet*. **1982**, *14*, 507.
(11) Ohta, T. *J. Phys. Chem*. **1983**, *87*, 1209.
(12) Siese, M.; Koch, R.; Fittschen, C.; Zetzsch, C. In *The Proceedings of Eurotrac Symposium '94*; Borrel, P. M., et al., Eds.; Academic Publishing bv: The Hague, 1994.
(13) Campuzano-Just, P.; Williams, M. B.; D'Ottone, L.; Hynes, A. J. *Geophys. Res. Lett*. **2000**, *27*, 693.
(14) Stevens, P.; L'Esperance, D.; Chuong, B.; Martin, G. *Int. J. Chem. Kinet*. **1999**, *31*, 637.
(15) Chuong, B.; Stevens, P. *J. Phys. Chem*. **2000**, *104*, 5230.
(16) McGivern, W. S.; Suh, I.; Clinkenbeard, A. D.; Zhang, R.; North, S. W. *J. Phys. Chem. A* **2000**, *104*, 6609.
(17) Zhang, R.; Suh, I.; Clinkenbeard, A. D.; Lei, W.; North, S. W. *J. Geophys. Res*. **2000**, *105*, 24627.
(18) Lloyd, A. C.; Atkinson, R.; Lurmann, F. W.; Nitta, B. *Atmos. Environ*. **1983**, *17*, 1931.
(19) Killus, J. P.; Whitten, G. Z. *Environ. Sci. Technol*. **1984**, *18*, 142.
(20) Arnts, R. R.; Gay, B. W., Jr. *Photochemistry of Some Naturally Emitted Hydrocarbons*; EPA-600/3-79-081, 1979.
(21) Atkinson, R.; Aschmann, S. M.; Tuazon, E. C.; Arey, J.; Zielinska, B. *Int. J. Chem. Kinet*. **1989**, *21*, 593.
(22) Gu, C. I.; Rynard, C. M.; Hendry, D. G.; Mill, T. *Environ. Sci. Technol*. **1985**, *19*, 151.
(23) Tuazon, E. C.; Atkinson, R. *Int. J. Chem. Kinet*. **1990**, *22*, 1221.
(24) Paulson, S. E.; Seinfeld, J. H. *Int. J. Chem. Kinet*. **1992**, *24*, 79.
(25) Grosjean, D., et al. *Environ. Sci. Technol*. **1993**, *27*, 830.
(26) Kwok, E. S.; Atkinson, R.; Arey, J. *Environ. Sci. Technol*. **1995**, *29*, 2467.
(27) Paulson, S. E.; Seinfeld, J. H. *J. Geophys. Res*. **1992**, *97*, 20703.
(28) Stevens, P. S.; Seymour, E.; Li, Z. *J. Phys. Chem*. **2000**, *104*, 5989.
(29) Lei, W.; Derecskei-Kovacs, A.; Zhang, R. *J. Chem. Phys*. **2000**, *113*, 5354.
(30) Jenkin M. E.; Hayman, G. D. *J. Chem. Soc., Faraday Trans*. **1995**, *91*, 1911.
(31) Frisch, M. J.; Trucks, G. W.; Schlegel, H. B.; Gill, P. M. W.; Johnson, B. G.; Robb, M. A.; Cheeseman, J. R.; Keith, T.; Petersson, G. A.; Montgomery, J. A.; Raghavachari, K.; Al-Laham, M. A.; Zakrzewski, V. G.; Ortiz, J. V.; Foresman, J. B.; Cioslowski, J.; Stefanov, B. B.; Nanayakkara, A.; Challacombe, M.; Peng, C. Y.; Ayala, P. Y.; Chen, W.; Wong, M. W.; Andres, J. L.; Replogle, E. S.; Gomperts, R.; Martin, R. L.; Fox, D. J.; Binkley, J. S.; Defrees, D. J.; Baker, J.; Stewart, J. P.; Head-Gordon, M.; Gonzalez, C.; Pople, J. A. *Gaussian 94*; Gaussian, Inc.: Pittsburgh, PA, 1995.
(32) Vibrational frequencies of the six peroxy radicals can be provided upon requested by interested readers.
(33) McGivern, W. S.; Derecskei-Kovacs, A.; North, S. W.; Francisco, J. S. *J. Phys. Chem*. **2000**, *104*, 463.
(34) *JANAF Thermochemical Tables*, 3rd ed.; Chase, M. W.; Davis, C. A.; Downey, J. R.; Frurip, D. J.; McDonald, R. A.; Syverud, A. N. Eds.; *J. Phys. Chem. Data, Suppl*. **1985**, 14.
(35) The conserved mode frequencies were also modeled by allowing them increase exponentially to the product frequencies. However, since the transition state is located far from the equilibrium bond distance, the difference from the product frequencies was found to be negligible.
(36) Hase, W. L. *Chem. Phys. Lett*. **1987**, *139*, 389.
(37) Andino, J. M.; Smith, J. N.; Flagan, R.; Goddard, W. A.; Seinfeld, J. H. *J. Phys. Chem*. **1996**, *100*, 10967.
(38) Gilbert, R. G.; Smith, S. C *Theory of Unimolecular and Recombination Reactions*; Blackwell Scientific: Oxford, UK, 1990.
(39) Lei, W.; Zhang, R.; McGivern, W. S.; Derecskei-Kovacs, A.; North, S. W. *Chem. Phys. Lett*. **2000**, *326*, 109.
(40) Peeters, J.; Boullart, W.; Hoeymissen, J. V. In *Proceedings of EUROTRAC Symposium '94*; Borrell, P. M., et al., Eds.; SPB Academic Publishers: The Hague, The Netherlands, 1994; p 110.
(41) Ruiz, R. P.; Bayes, K. D. *J. Phys. Chem*. **1984**, *88*, 2592.
(42) Paltenghi, R.; Ogryzlo, E. A.; Bayes, K. D. *J. Phys. Chem*. **1984**, *88*, 2595.
(43) Ebata, T.; Obi, K.; Tanaka, I. *Chem. Phys. Lett*. **1981**, *77*, 480.
(44) Since our calculations show substantially different rate constants for O_2 addition to individual OH−isoprene products, a direct comparison to experiments which attempt to fit the inherently complex kinetics using a single rate constant is not straightforward. We have performed kinetics simulations in order to find the best single effective rate constant consistent with our calculated rate constants and the branching ratios of the OH−isoprene adducts (ref 16). We obtain a value of 1.75×10^{-12} cm^3 $molecule^{-1}$ s^{-1} in this manner.
(45) Cobos, C. J.; Hippler, H.; Luther, K.; Ravishankara, A. R.; Troe, J. *J. Phys. Chem*. **1985**, *89*, 4332.
(46) Knyazev, V. D.; Slagle, I. R. *J. Phys. Chem*. **1998**, *102*, 1770.
(47) Miyoshi, A.; Matsumi, H.; Washida, N. *J. Phys. Chem*. **1990**, *94*, 3016.
(48) Bohn, B.; Zetzsch, C. *Phys. Chem. Chem. Phys*. **1999**, *1*, 5097.
(49) Knispel, R.; Koch, R.; Siese, M.; Zetzsch, C. *Ber. Bunsen-Ges. Phys. Chem*. **1990**, *94*, 1375.
(50) Stark, M. S. *J. Am. Chem. Soc*. **2000**, *122*, 4162.
(51) Diaz-Acosta, I.; Alvarez, J. R.; Vivier-Bunge, A. *Int. J. Chem. Kinet*. **1999**, *31*, 29.
(52) Garcia-Cruz, I.; Castro, M.; Vivier-Bunge, A. *J. Comput. Chem*. **2000**, *21*, 716.
(53) Ghigo, G.; Tonachini, G. *J. Am. Chem. Soc*. **1998**, *120*, 6753.
(54) Jenkin, M. E.; Murrells, T. P.; Shalliker, S. J.; Hayman, G. D. *J. Chem. Soc., Faraday Trans*. **1993**, *89*, 433.
(55) Koch, R.; Siese, M.; Fittschen, C.; Zetzsch, C. In A Contribution to the EUROTRAC subproject LACTOZ, 1995; p 268.